Chapter

Wax Chemical and Morphological Investigation of Brazilian Crude Oils

Erika C.A. Nunes Chrisman, Angela C.P. Duncke, Márcia C.K. Oliveira and Márcio N. Souza

Abstract

The waxes in petroleum can precipitate and form unwanted gels and deposition when exposed to low temperatures. The idea of this chapter is to approach methods of quantification and physicochemical and morphological characterization of waxes and how this information can help in understanding this deposition. Information such as the quantity of waxes and the chemical structures in the oil is fundamental to predict the possible deposition and its ability to aggregate with other crystals. For example, the knowledge about the wax morphology may contribute to explain the nucleation and growth of the deposits. The polarized light microscopy, the most common technique to visualize wax crystals, and the bright-field microscopy, the most simple technique, able to show crystal details that have not been seen on the polarized light, was used.

Keywords: waxes, crude oil, quantification, characterization, microscopy, DSC

1. Introduction

Petroleum is a complex mixture of hydrocarbons of varying nature and small fractions of nitrogen, oxygen, sulfur, and metal compounds. At room temperature, petroleum can be gas, liquid, and/or solid, being considered as gases and solids dispersing in a liquid phase [1]. Under high temperature and pressure, as encountered at reservoirs (e.g., 8000–15,000 psi and 70–150°C), Newtonian rheological behavior prevails, whereas at low temperatures the pseudoplastic behavior is commonly found [2].

A large portion of the Brazilian oil production comes from offshore fields, from the pre-salt layer. These oils have high levels of waxes, which are alkanes (linear or branched) encompassing carbonic chains of 15–75 carbons [3, 4]. This class of compounds has a high precipitation potential, due to the low sea temperatures (about 4–5°C) [5–7]. In temperatures below the wax appearance temperature (WAT), the wax crystallization takes place with subsequent deposition [2]. The wax deposition is dominated by the molecular diffusion mechanism [8] in which the waxes initially precipitate at the cold pipeline walls and subsequently generate a radial gradient of precipitation causing deposit [9, 10]. This can lead to a strong waxy crystal interlocking network, which causes pipeline clogs and dramatically affects the rheological fluid behavior [9, 11–13].

Gelation and deposition problems, leading to increases in yield stress and losses in production, are probably connected to wax morphology. This chapter aims to show some techniques to characterize the structure and morphology of wax crystals based on four pre-salt Brazilian crude oils, all provided by Petrobras, under different shear conditions, aging times, and temperatures. In addition, some physicochemical characterization techniques are discussed as density, viscosity, and SAP (saturated, aromatic, and polar). The wax quantification is the harder part of the study of crude oils, due to the petroleum complex matrix, which can cause complications related to the wax crude oil separation; however, through differential scanning calorimeter (DSC) measurements, it is possible to obtain a precipitated wax content as well as through some American Society for Testing and Materials (ASTM), Universal Oil Products Collection (UOP), gas chromatography (GC), and others.

2. Morphological characterizations

Due to the petroleum multicomponent nature, the wax precipitation occurs heterogeneously, and resins and asphaltene molecules, inorganic solids, and corrosion products, among others, can behave as nuclei for the phenomenon, enhancing the flow assurance issue [14].

Waxes crystallize into basically orthorhombic and hexagonal shapes. The orthorhombic form is needle-shaped, and it is found in crudes with high waxy content [15, 16]. Crystallization kinetics and crystal morphology can be highly affected by some recognized factors, such as cooling rate [13, 17–23], carbonic chain nature (branched or linear and average length) [21], resins and asphaltene content [2, 7, 24, 25], and shear rate [16, 26–28].

The polarized light (PL) optical microscopy is the fundamental technique for wax crystal examination [24]. According to [29] it allows verifying the anisotropic optical behavior of crystalline materials, named birefringence. This technique uses two cross polarizers. When the light beam passes through crystalline structures, as wax crystals, the polarized light plane is altered generating a visible image pattern. On the other hand, isotropic structures, which do not exhibit the same level of organization, are not able to modify the light plane. Apart from PL microscopy, the bright-field (BF) microscopy regards another important technique for wax crystal visualization. The procedure is very simple, and no artifacts are employed in the optical path.

Figure 1 shows BF and PL micrographs of P1 Brazilian crude oil, for the same point of the coverslip, at 25°C, as received, i.e., without any thermal treatment. All

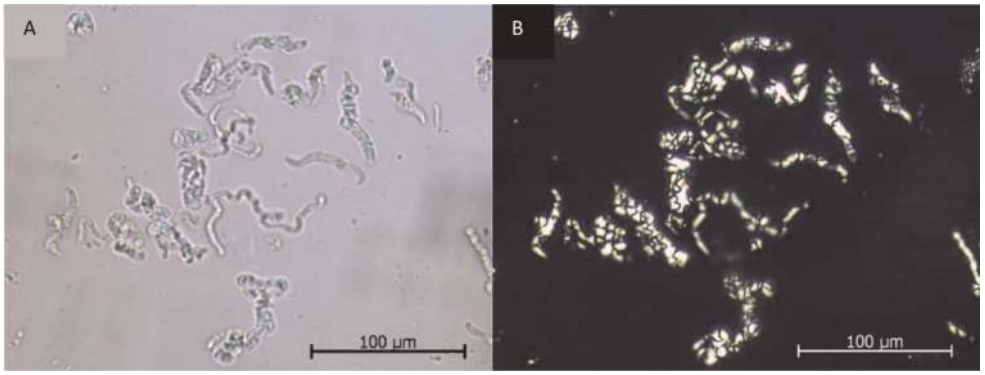

Figure 1.
(A) BF and (B) PL micrograph of P1, for the same point of cover slip at 25°C, as received.

the aliquots of crude oil in this chapter were observed on optical microscope Axio Vert 40 MAT (Carl Zeiss).

The BF technique (**Figure 1a**) provides lower contrast than PL technique (**Figure 1b**); however, it can be seen that in BF micrographs the wax crystal is continuous, i.e., the structure appears and integrates, without rupture. On the other hand, PL micrographs show "dark cracks," i.e., the wax crystals do not appear entirely. These "dark cracks" can be attributed to two factors: first, amorphous or low crystallinity regions due to the presence of impurities and second, due to light extinction positions, related to the parallel orientation of polarizers and the crystal organization, i.e., no light is deflected by the sample [30]. Therefore, much attention should be taken to make length measurements in crystals observed by PL technique. According to these results, to determine the size and crystal shape (as verified by BF) can be critical to avoid erroneous measurements. In this work, the length measurements were performed on images obtained by BF, but the PL images are shown due to easy observation.

Another characteristic of wax crystals that can be seen in **Figure 1a** is a roughened surface. The roughness, as well as the tortuosity of wax crystals, can be attributed to a heterogeneous nucleation and growth, by the presence of asphaltenes, resins, and different wax chain lengths or the presence of isocycle [24, 31].

In order to characterize the wax morphology and crystals length in dependence of temperature and shear, a continuous cooling protocol was performed (**Figure 2**). Initially, the thermal history removal of 100 mL of each oil was carried out by heating the samples for 2 h at 80°C in a circulating oven model 400-3ND (Ethik Technology). This condition is sufficient to dissolve all wax present in the crude oil and prevent that the wax crystal formation was not influenced by pre-existing nuclei [32, 33]. Secondly, the samples were transferred to a jacketed Becker coupled to a circulation bath (Haake Phoenix II-C25P - Thermo Scientific). Then, the cooling step was carried out quiescently or in presence of shear (mechanical agitation 250 rpm on RW20 Digital IKA) for 80–5°C. The cooling rate was 0.5°C/min. **Figure 2** shows the influence of shear on waxy crystal growth of P1–P4 paraffinic oil comparing the PL micrographs of tests carried out at 5°C, on quiescent and shear cooling conditions.

It was verified that experiments performed with quiescent condition (**Figure 2A–D**) were characterized by large crystals and cluster of crystals when compared with experiments carried out with shear condition (**Figure 2E–H**). The

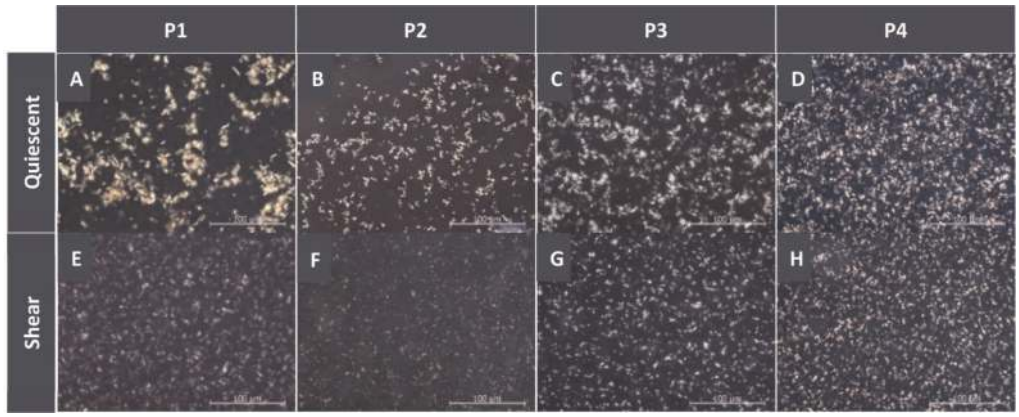

Figure 2.
PL micrographs of test performed at 5°C on quiescent (A–D) and shear (E–H) conditions of waxy crude oils P1–P4.

researchers carried out by [2, 16, 34] show that under quiescent conditions, the waxy crystals were characterized by extended and continuous particles. The formation of extended and continuous particles allowed a colloidal network that embodies the oil itself. Probably, the gel would have a high shear modulus, in order to the side-by-side interactions between particles. Under the shear condition, the lateral growth of the individual crystals is constricted. However, extended particles are not observed, and consequently, these particles lost their interconnectivity.

The wax crystals presented in waxy crude oils (**Figure 2**) are elongated. According to [16], waxes precipitated in crude oil tend to crystallize in an orthorhombic structure, which is characterized by an elongated structure. Evidently, the crystals of **Figure 2** (and in detail in **Figure 1**) are not linear (needle-like). The sinuosity and tortuosity are probably due to the presence of impurities during nucleation and crystal growth processes [2, 21]. [2] analyzed the aspect ratio, which is the ratio between the length and the width of a crystal. Based on aspect ratio value, it is possible to verify how the structure is elongated. The values of average aspect ratio, at 5°C, of samples P1, P2, and P3, are 5.5, 6.2, and 5.0, respectively, legitimizing the elongated characteristic. P4 sample has a 4.0 aspect ratio value, which indicates that the crystals are less elongated than other samples.

Table 1 shows the average length and width of crystals to waxy crude oils P1–P4 in function of temperature for 30, 10, and 5°C, for quiescent and shear conditions, and shows the average percentage of crystal growth between both cooling conditions.

For quiescent conditions, it is possible to note the crystal length increases between 10 and 5°C; however, for shear conditions, the length becomes basically stationary at these temperatures. This behavior could be attributed to a possible crystal breakage by the shear, which prevents the crystals from becoming large. The average percentage of growth between quiescent and shear conditions increases with the temperature decrease. For 30°C the crystals obtained in quiescent cooling are about 12.4% higher than that obtained by shear conditions. At 5°C this difference reaches 25.1%. On the other hand, the crystal width underwent an effective action of the shear, being about 22.3% less wide than those obtained in quiescent conditions.

To illustrate the **Table 1**, **Figure 3** shows PL micrographs of P3 obtained at 30, 10, and 5°C during quiescent cooling. This condition resembles the operational shutdowns when crude oil is cooled. As expected and discussed above, the concentration and size of wax crystals increase with the decrease in temperature. Since the solubility of high molecular weight waxes decreases sharply with the decrease in temperature, they precipitate out and crystallize. This result indicates that in low temperatures, it is more probably to have problems of flow assurance due to pipeline blockage occasioned by wax crystal depositions and to the formation of a high-strength gel, characterized by yield stress [35–37].

	T	P1		P2		P3		P4		Average Growth
	(°C)	Quiescent	Shear	Quiescent	Shear	Quiescent	Shear	Quiescent	Shear	(%)
Length (μm)	30	12.0	8.3	6.2	5.3	10.2	10.0	8.2	8.0	12.4
	10	14.6	12.7	14.6	9.0	13.3	11.3	9.6	8.9	18.4
	5	16.2	12.8	14.9	8.9	15.4	11.3	10.4	9.1	25.1
Width (μm)	30	2.3	1.5	2.4	1.5	2.3	1.9	2.2	2.0	24.7
	10	3.0	2.5	2.7	1.8	3.2	2.6	2.6	2.3	20.0
	5	3.1	2.4	2.9	1.9	3.3	2.6	2.7	2.4	22.3

Table 1.
Length and width of crystal's average and growth percentage.

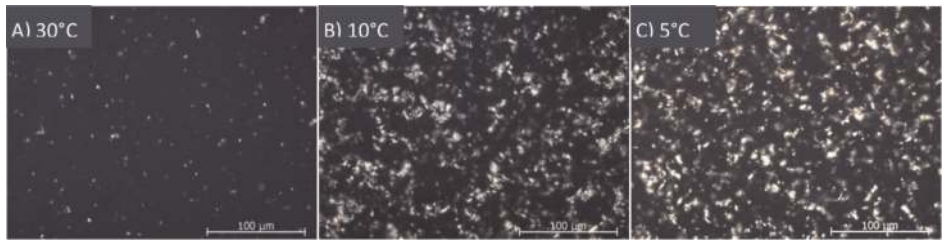

Figure 3.
PL micrographs of P3 obtained at (A) 30°C, (B) 10°C, (C) 5°C and during quiescent cooling.

Another common factor studied on precipitation and morphology of waxy crystals is the aging time, which represents the influence of the time at a certainly constant temperature on the crystal wax. PL micrographs in **Figure 4** show the influence of 1 h aging time at temperatures 40, 20, and 5°C, for P4. To study the aging time influence, first, the thermal history was removed. The samples were transferred to the jacketed Becker coupled to a circulation bath at 80°C and then started the cooling steps (80–40°C; 80–20°C or 80–5°C). When the temperature arrives 40, 20, or 5°C, the samples were kept cool for 1 h at this temperature. The cooling rate was 0.5°C/min.

It was verified that the aging time favored the increase of crystal length and appearance of large clusters. This result can be attributed to the Ostwald ripening of wax crystals, a mechanism by which the large crystals grew at the expenses of smaller crystals of higher energy. Furthermore, oil uptake can also change the wax crystal distribution, leading to larger and softer wax crystals that can interpenetrate increasing intermolecular interactions between crystals [11, 37, 38].

Table 2 shows the wax crystal's average length at t = 0 h and after 1 h (t = 1 h) at temperatures 40, 20, and 5°C, as well as the crystal growth percentage in function of aging time.

Analyzing **Table 2**, at 40°C the oils P1 and P3 show an increase of about 26.3% in the length of the crystal after 1 h in an isothermal condition. Under these same conditions, P2 shows a growth of almost 80.0%. P2 has the WAT at 42.1°C (see 4. Wax quantification), and consequently, there is no visible crystal on microscope when the temperature just arrives at 40°C. For this reason, the crystal size, in this

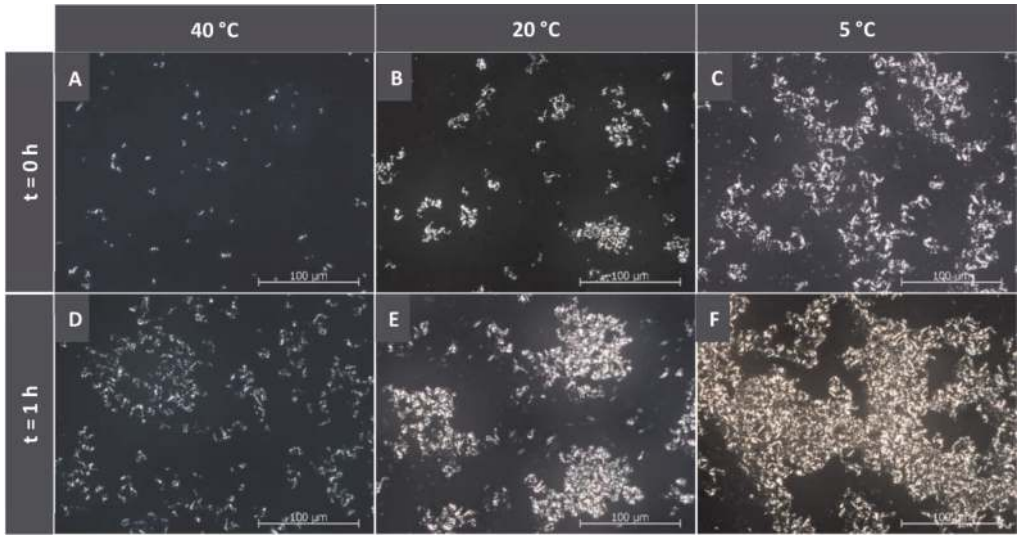

Figure 4.
PL micrographs of tests carried out with P4, at t = 0 h for 40°C (A), 20°C (B) and 5°C (C); and after 1 h at 40°C (D), 20°C (E) and 5°C (F).

Oil	40 °C			20 °C			5 °C		
	t = 0 h (μm)	t = 1 h (μm)	Growth %	t = 0 h (μm)	t = 1 h (μm)	Growth %	t = 0 h (μm)	t = 1 h (μm)	Growth %
P1	8.2	11.2	26.7	13.0	15.9	17.8	16.1	18.3	12.4
P2	*	4.8	79.0	7.3	10.2	28.1	15.5	17.2	9.6
P3	7.9	10.6	26.0	11.5	14.3	19.6	15.1	16.1	6.1
P4	4.9	8.9	45.5	9.3	12.6	26.0	10.7	12.3	13.2

** No crystals were present. The crystal size of 1.0 μm was convened because it is the detection limit of the microscope.*

Table 2.
Average wax crystal length at t = 0 h and t = 1 h at 40, 20, and 5°C and crystal's growth percentage.

case, was considered 1.0 μm, the microscope detection limit. However, after 1 h at 40°C, this sample presents small crystals of about 4.8 μm. Evaluating a percentage of growth at 20 and 5°C, a reduction is noticed. The wax crystals seem to grow more significantly at elevated temperatures. In t = 0 at 5°C, the wax crystal has a large size due to the temperature decrease, and after 1 h in an isothermal condition, the wax crystal grows little, i.e., its sizes do not "double" as at 40°C. A smaller variation was noted between the sample growth percentages at 5°C. This temperature is close to that observed in the production fields. After 1 h at 5°C, the wax crystals are 10.3 ± 2.8% higher than when the temperature just arrives 5°C. Generalizing this information and transferring it to offshore production fields, after a 1-h stop with the oil at 5°C, the crystals can grow about 10%. Of course, this is a hypothetical condition because it is impossible to happen, since the cooling rate in the fields is smaller than that used in this study, which can result in greater wax crystals.

3. Physicochemical characterization

Due to the complex matrix that is the petroleum itself, the physicochemical characterization is very relevant in order to address a proper comparison between the microscopic images, which is a very useful tool in the wax crystal morphology study. The most common physicochemical characterization techniques are:

- Density: measured mainly by ASTM-D7042. By density (at 60°F = 15.6°C) it is possible to obtain the °API following Eq. (1). °API is the most general classification at petroleum industry:

$$^{\circ}API = \frac{141.5}{\rho} - 131.5 \quad (1)$$

- Viscosity: can be also determined by ASTM-D7042 on a viscometer or by rheological tests.

- Saturated, aromatic, resin, and asphaltene (SARA): can be determined mainly by Clay-Gel, according to ASTM D2007, thin layer chromatography with flame ionization detection (TLC-FID) according to IP-469, or by high-performance liquid chromatography (HPLC) according to IP-368. In this work, SARA content was obtained by TLC-FID using the IATROSCAN MK-6 (NTS International), for all paraffinic crude oils.

- SAP: this characterization is less specific than SARA because resins and asphaltenes are considered together as polars. The SAP contents were determined by a liquid chromatography separation composed by silica gel column 60 (2.5 g silica, 0.063–0.200 mm) from Merck, which was used to determine the SAP content. The column was heated for 10 hrs at 120°C for activation. Fractions were eluted with 10 mL n-hexane for saturated, 10 mL of n-hexane/dichloromethane (8:2) for aromatic, and dichloromethane/methanol (9:1) for polar fractions. Residual solvents were submitted to a rotary evaporation. This technique was employed only for non-paraffinic (NP).

- WAT: this is one of the main characterizations when working with waxy crudes, because it gives an idea of the precipitation potential of the oil and ideas about the wax type. A wide range of techniques can be used to determine WAT, as microscopy, rheology, and near-infrared spectroscopy (NIR), but the most used is DSC. In this work, measurements were performed using Nano DSC differential scanning calorimeter (TA Instruments). The samples were heated from room temperature to 80°C, at 2°C/min. Then they were held for 15 min at 80°C, following by a cooling step from 80–4°C, at 0.5°C/min. Kerosene was used as the reference. Before measurements, samples were homogenized and kept under vacuum for degasification for at least 30 min. A volume of 300.0 μL of crude was used.

- Gas chromatography: this technique is employed to characterize the carbon number distribution of petroleum waxes and the normal and non-normal hydrocarbons. It is oriented by ASTM D5442-17. In this work the GC evaluated the carbon distribution up to C36.

Table 3 presents some physicochemical characterization of the four paraffinic P1–P4 and NP oils used as reference of wax absence, also provided by Petrobras. All crude oils have relatively similar values of density. The paraffinic samples are considered medium oils, while NP is classified as heavy oil according to the °API scale. The viscosity varies greatly between samples, with P1 and P3 being the less viscous. P4 exhibits the highest viscosity at 20°C, being 100 times greater than the lower one (P3). Non-paraffinic petroleum classified as heavy oil also has high viscosity (896.8 mPa.s).

WAT is defined as the onset temperature, that is, the intersection point of the baseline and the tangent line of the inflection point of the exothermic peak [4, 39, 40]. In crude oils, it is common to observe two exothermic events (peaks). WAT depends on the concentration and molecular weight of waxes and the chemical characterization of hydrocarbon matrix [41]. Due to the oil complexity, the

Oil	ρ (g/cm³)	°API	μ (mPa.s)	WAT (°C)		Oil Composition (wt. %)			
				1° event	2° event	Sat.	Aro.	Res.	Asp.
P1	0.88	28.2	153.6 ± 1.1	46.6	25.7	54.0	24.0	22.0	<0.50
P2	0.91	23.3	427. ± 1.0	42.1	23.5	53.1	25.6	21.1	<0.17
P3	0.89	27.2	113.3 ± 1.3	46.8	25.0	63.1	18.2	18.6	<0.50
P4	0.91	23.6	11279.3 ± 178.9	53.1	29.4	40.4	16.2	42.7	0.65
NP	0.93	19.4	896.8 ± 2.5	37.9	19.2	57.6	28.9	13.4*	

*SAP - polars

Table 3.
Physicochemical characterizations.

values of the peaks are around 50°C for the first exothermic event and 25°C for the second; [16, 42] assign the first peak to a liquid-liquid transition and the second to liquid-solid transition. However, in this paper, the authors believe that each exothermic event refers to a different group of waxes according to the chain length. [43, 44] declare that n-alkanes with similar carbon numbers can co-crystallize with the longer n-alkane chains.

Figure 5 shows the thermal curves for all samples obtained by Nano DSC. All oils have at least two well-defined exothermic peaks. It is possible to note a great similarity between the WAT values and the intensity of the exothermic peaks in the curves of the oils P1 and P3. However, the saturated values are quite different (**Table 3**). P1 has the 54.0 wt% and P3 has the 63.1 wt%, the highest values between the samples. Nevertheless, we must keep in mind that not all saturated content refers to wax; thus, these differences between saturated content among the oils do not represent the real wax content.

Continuing the analysis of **Figure 5**, it is noted that P2 was characterized by the lower WAT values and P4 shows the higher (**Table 3**), which may be an evidence that the P2 is composed by short waxy chains and P4 has the longest. According to [36] the larger the carbon chain size, the higher the crystallization temperature. Moreover, the first peak of P2 is barely evident which can be a sign of less wax content. P4 has a second peak very evident, that is, this oil may contain the higher wax content. However, P4 has the smallest crystals, as discussed before, being on average 35% smaller than the others are. According to the P4 higher WAT value, large crystals were expected. Senra et al. [45] suggest a co-crystallization between chains with different carbon numbers and with other compounds, affecting the crystal morphology. According to [46] the co-crystallization weakens the crystal structure and disfavors large crystal formation. This is a plausible hypothesis, since according to SARA, P4 has 42.7 wt% of resins and the higher content of asphaltenes (0.65 wt%).

Another curious fact is a possible third peak at temperatures just below the second, especially for P2 and P4. This peak may represent a third population of waxes, and as far as we know, it was never reported in conventional DSC analyses. Possibly this third peak is related to a group of very-short-chain waxes. Based on this observation, it is verified that the Nano DSC technique presents greater sensitivity to enthalpy variations. In the conventional DSC technique, this third peak may be masked with the second. According to [19] the conventional DSC is not

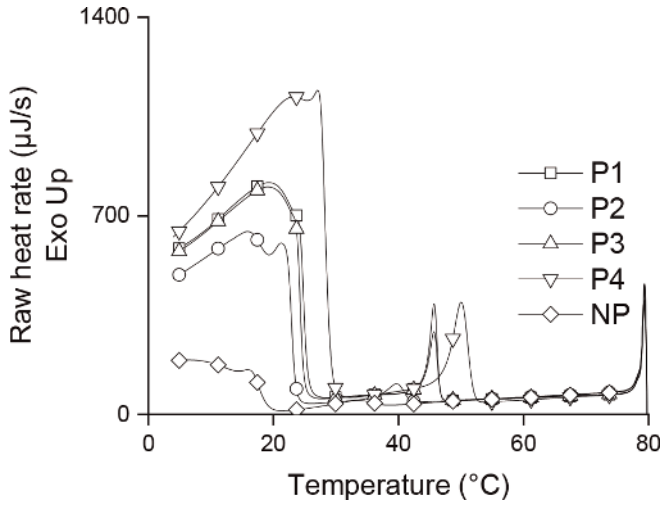

Figure 5.
P1-P4 and NP thermal curves behavior.

sufficiently sensitive to identify WAT for samples with low wax contents; however, the Nano DSC shows two slight baseline variations for NP sample, even in a low cooling rate (0.5°C/min). These peaks are very low if compared to other oils due to the non-paraffinic characteristic of NP, but their presence confirms the sensitivity of the equipment.

Figure 6 shows the GC graphs of the crude oils P1–P4 and their respective extracted waxes through the UOP46–85 method (see Section 4). It is possible to note that the values obtained for the GC of the crude oil (white bars) are dispersed

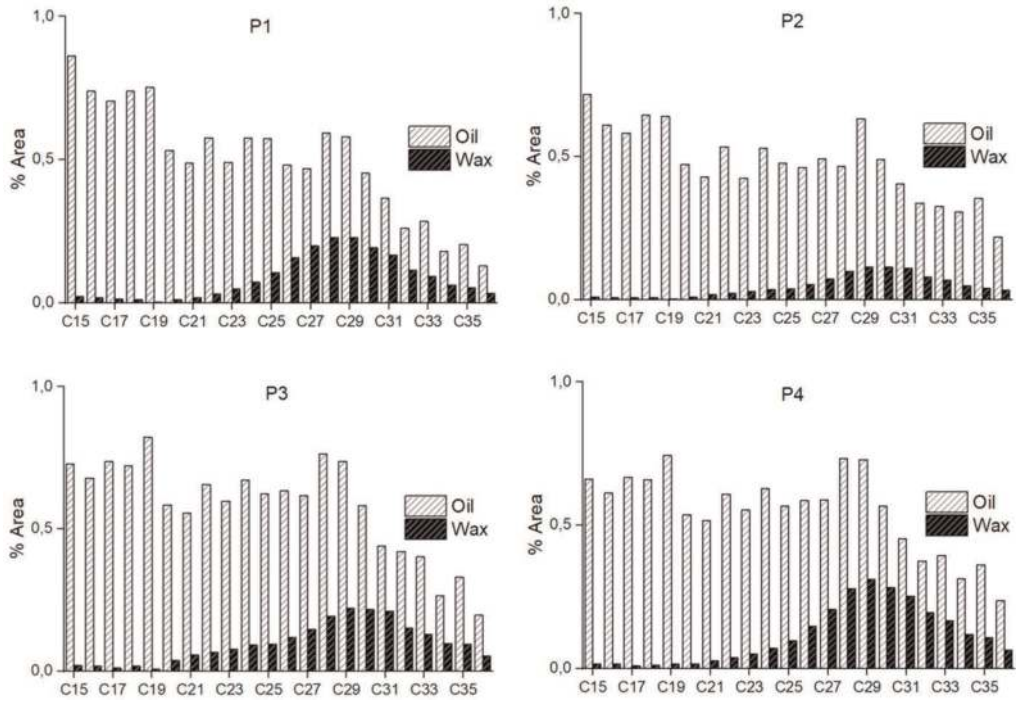

Figure 6.
Carbon number distribution for P1-P4 crude oil.

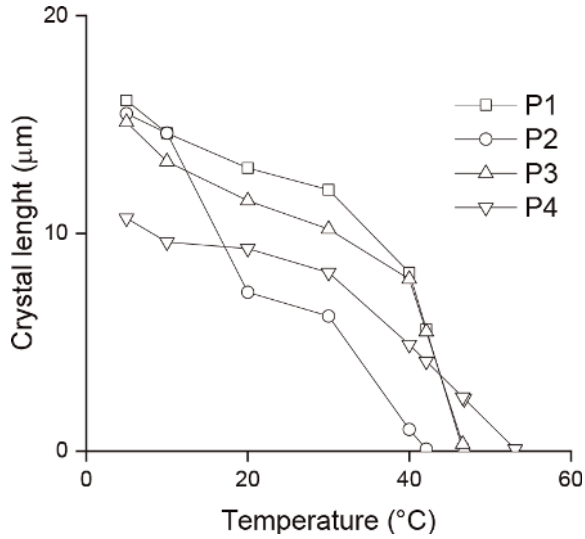

Figure 7.
P1-P4 crystal length versus temperature.

and have a tendency of decrease after around C30. This behavior can be attributed to the complex matrix of the oil itself. However, the carbon distribution number obtained from the extracted wax fraction from each oil (dark bars) has a more plausible chain distribution. For all oils, there is a chain predominance around C30.

Figure 7 shows the crystal length versus temperature for P1–P4. The first experimental point of the curves is the respective WAT values. This graph is presented in order to analyze the growth tendency of the wax crystals as a function of the temperature reduction, as a way to summarize the information previously discussed.

4. Wax quantification

The wax quantification is more difficult to develop than the other characterizations. However, some techniques are available:

- GC: as mentioned on 3. Physicochemical characterization, this technique is employed to characterize the carbon number distribution. In this work the GC evaluated the carbon distribution up to C36.

- Nuclear magnetic resonance (NMR) correlation: presented by [47], estimates the wax content of crude oil and their fractions by H NMR spectroscopy. The method shows good fit for oils with boiling range from 340 to 550°C.

- UOP 46–85 method: estimates the wax content of the crude oil and is defined as the mass percentage of precipitated material when an asphaltene-free sample solution is cooled to −30°C.

- DSC integration baseline: is possible to obtain the total thermal effect of the wax precipitation (Q) by integrating the area of the exothermic peaks. With this value, the wax precipitated concentration (c_w) can be determined following Eq. 2 [48]. $\overline{Q}$ is defined as 210 J/g, a constant thermal value of wax precipitation for crude oils with an unknown molecular structure [49]. WAT is the WAT temperature itself, and T_f is the final temperature, in this work, 4°C:

$$c_w = \frac{\int_{T_f}^{WAT} dQ}{\overline{Q}} = \frac{Q}{\overline{Q}} \tag{2}$$

By means of simple math, it is possible to calculate the mass content of precipitated waxes (w) as shown in Eq. (3), where ρ is the specific mass and V_e is the experimental volume used to the DSC measurement:

$$w = \frac{c_w}{\rho . V_e} .100 \tag{3}$$

The percentages by mass of precipitated wax obtained by the DSC integration baseline show 3.1 and 2.9 wt% for P1 and P3, respectively. As cited before these oils have many similarities. P2 has the lowest value (2.2 wt%) and P4 has 4.7 wt% of precipitated waxes. However, by the UOP 46–85 method, the wax contents in mass percentage obtained were 3.7 ± 0.3 for P1, 5.7 ± 0.4 for P2, 5.0 ± 0.1 for P3, and 3.6 ± 0.2 for P4. In general, these values are at the same range of the values

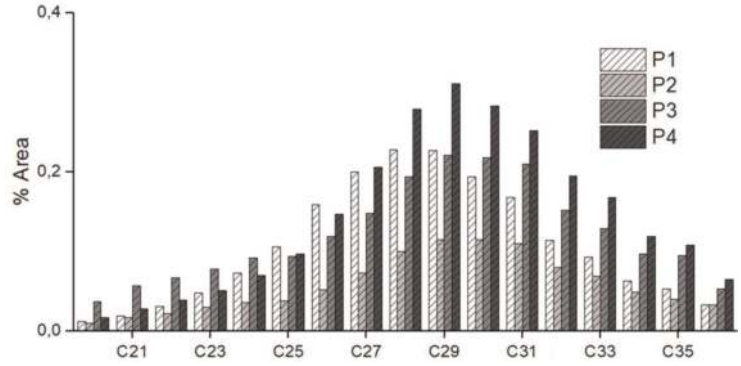

Figure 8.
Carbon number distribution for P1-P4 crude oil.

obtained by DSC integration baseline, but they are not in agreement with the values obtained by this same technique. The UOP 46–85 method is a traditional way of wax estimation by very steps extractions, as well as time-consuming, lots of chemicals and solvents. These many delicate steps have great chances to produce erroneous results if not done properly [47].

Figure 8 shows the carbon number distribution, obtained through GC, only for the extracted waxes by means of UOP method. As determined by DSC integration baseline, P2 has the lowest percentage of waxes, and P4 has the highest. This can be observed again on the GC graph. According to [50] the GC and DSC analyses can be used to quantify wax content of crude oils showing reasonable agreement, but wax precipitation technique, as UOP method, must be corrected due to the presence of trapped crude oil in the precipitated solid wax crystal.

5. Conclusions

The polarized light microscope is the most used technique to visualize wax crystals; however, bright-field microscopy shows crystal details that are not seen on the polarized light. The wax crystals observed have elongated structure, but they are not linear, i.e., not needle-shaped. They have superficial roughness attributed to the presence of crystallization interferers such as asphaltenes, resins, organic solids, and different carbon chain sizes. The gradual temperature decrease favors the length crystal increases, as well as the increase in the quantity and size of the agglomerates. Under shear conditions, crystals were observed around 25% smaller and in less quantity than under quiescent conditions. In addition, shearing promotes crystal breakage at very low temperatures. The aging time of the oil favors the crystal growth more drastically at higher temperatures (around 45% after 1 h at 40°C) than in low temperatures (around 10% after 1 h at 5°C), as well as the formation of agglomerates. P4 shows the higher content of precipitated waxes by means of DSC integration baseline and GC analysis, but their crystals were smaller, possibly due to the higher polar content. The DSC integration baseline is in accordance to the GC result to wax content determination; however, the UOP method is in disagreement. Another characteristic observed about Nano DSC was the great sensitivity to obtain WAT values. This technique can identify a possibly third peak precipitation and two peaks for the NP sample.

This chapter looks at some techniques of wax characterization and quantification; however, there are many other techniques that can be used and that present satisfactory results. The use of combined techniques may assist in the more accurate analysis of sample characteristics.

Acknowledgements

The authors thank Conselho Nacional de Pesquisa e Desenvolvimento (CNPq), Fundação Carlos Chagas de Amparo à Pesquisa do Estado do Rio de Janeiro (FAPERJ), and Petrobras for supporting this work.

Conflict of interest

The authors declare no competing financial interest.

Nomenclatures

API	American Petroleum Institute
ASTM	American Society for Testing and Materials
BF	brightfield
DSC	differential scanning calorimeter
GC	gas chromatography
HPLC	high performance liquid chromatography
NIR	near-infrared spectroscopy
NMR	nuclear magnetic resonance
NP	non-paraffinic
$P_{1–4}$	paraffinic petroleum
PL	polarized light
SAP	saturated, aromatic and polar
SARA	saturated, aromatic, resins and asphaltenes
TLC-FID	thin layer chromatography with flame ionization detection
UOP	universal oil products collection
WAT	wax appearance temperature
Q	total thermal effect of wax precipitation
c_w	wax precipitated concentration
$\overline{Q}$	constant thermal value of wax precipitation
T_f	final DSC temperature
w	mass content of precipitated waxes
ρ	specific mass
V_e	experimental volume used to the DSC measurement

DOI: http://dx.doi.org/10.5772/intechopen.83736

Author details

Erika C.A. Nunes Chrisman[1*], Angela C.P. Duncke[1], Márcia C.K. Oliveira[2] and Márcio N. Souza[1]

1 Federal University of Rio de Janeiro, Rio de Janeiro, Brazil

2 Cenpes, Petrobras, Rio de Janeiro, Brazil

*Address all correspondence to: enunes@eq.ufrj.br

References

[1] Farah MA. Petróleo e seus derivados: definição, constituição, aplicação, especificações, características de qualidade. Rio de Janeiro: LTC; 2012. 261 p

[2] Venkatesan R, Nagarajan NR, Paso K, Yi Y-B, Sastry AM, Fogler HS. The strength of paraffin gels formed under static and flow conditions. Chemical Engineering Science. 2005;**60**:3587-3598. DOI: 10.1016/j.ces.2005.02.045

[3] Hammami A, Raines MA. Paraffin deposition from crude oils: Comparison of laboratory results with field data. SPE Journal. 1999;**4**(1):9-18. DOI: 10.2118/54021-PA

[4] Kok MV, Varfolomeev MA, Nurgaliev DK. Wax appearance temperature (WAT) determinations of different origin crude oils by differential scanning calorimetry. Journal of Petroleum Science and Engineering. 2018;**168**:542-545. DOI: 10.1016/j.petrol.2018.05.045

[5] Lopes RT, Valente CM, De Jesus EFO, Camerini CS. Detection of paraffin deposition inside a draining tubulation by Compton scattering technique. Applied Radiation and Isotopes. 1997; **48**(10):1443-1450. DOI: 10.1016/S0969-8043(97)00255-8

[6] Azevedo LFA, Teixeira AM. A critical review of the modeling of wax deposition mechanisms. Petroleum Science and Technology. 2003;**21**(3–4): 393-408. DOI: 10.1081/LFT-120018528

[7] Huang Z, Lee HS, Senra M, Fogler HS. A fundamental model of wax deposition in subsea oil pipelines. AICHE Journal. 2011;**57**(11):2955-2964. DOI: 10.1002/aic.12517

[8] Creek JL, Lund HJ, Brill JP, Volk M. Wax deposition in single phase flow. Fluid Phase Equilibria. 1999;**158**: 801-811. DOI: 10.1016/S0378-3812(99)00106-5

[9] Quan Q, Gong J, Wang W, Gao G. Study on the aging and critical carbon number of wax deposition with temperature for crude oils. Journal of Petroleum Science and Engineering. 2015;**130**:1-5. DOI: 10.1016/j.petrol.2015.03.026

[10] Zheng S, Fogler HS. Fundamental investigation of wax diffusion characteristics in water-in-oil emulsion. Industrial and Engineering Chemistry Research. 2015;**54**:4420-4428. DOI: 10.1021/ie501955e

[11] Lin M, Li C, Yang F, Ma Y. Isothermal structure development of Qinghai waxy crude oil after static and dynamic cooling. Journal of Petroleum Science and Engineering. 2011;**77**: 351-358. DOI: 10.1016/j.petrol.2011.04.010

[12] Eskin D, Ratulowski J, Akbarzadeh K. A model of wax deposit layer formation. Chemical Engineering Science. 2013;**97**:311-319. DOI: 10.1016/j.ces.2013.04.040

[13] Kasumu AS, Arumugam S, Mehrotra AK. Effect of cooling rate on the wax precipitation temperature of "waxy" mixtures. Fuel. 2013;**103**:1144-1147. DOI: 10.1016/j.fuel.2012.09.036

[14] Allen TO, Roberts AP. Production Operations: Well Completions, Workover, and Stimulation. 3rd ed. Vol. 2. Tulsa: Inc.; 1989. 364 p

[15] Srivastava SP, Tandon RS, Verma PS, Saxena AK, Joshi GC, Phatak SD. Crystallization behavior of n-paraffins in Bombay-High middle-distillate wax/gel. Fuel. 1992;**71**:533-537. DOI: 10.1016/0016-2361(92)90150-M

[16] Kané M, Djabourov M, Volle J-L, Lechaire J-P, Frebourg G. Morphology of paraffin crystals in waxy crude oils cooled in quiescent conditions and under flow. Fuel. 2003;**82**:127-135. DOI: 10.1016/S0016-2361(02)00222-3

[17] Hammami A, Mehrotra AK. Thermal behavior of polymorphic n-alkanes: effect of cooling rate on the major transition temperatures. Fuel. 1995;**74**:96-101. DOI: 10.1016/0016-2361(94)P4338-3

[18] Cazaux G, Barre L, Brucy F. Waxy crude cold start: Assessment through gel structural properties. In: SPE Annual Technical Conference and Exhibition, 27–30 September 1998; New Orleans. Louisiana: Society of Petroleum Engineers; 1998. pp. 729-739. DOI: 10.2118/49213-MS

[19] Jiang Z, Hutchinson JM, Imrie CT. Measurement of the wax appearance temperatures of crude oils by temperature modulated differential scanning calorimetry. Fuel. 2001;**80**: 367-371. DOI: 10.1016/S0016-2361(00)00092-2

[20] Guo X, Pethica BA, Huang JS, Adamson DH, Prud'homme RK. Effect of cooling rate on crystallization of model waxy oils with microcrystalline poly(ethylene butene). Energy & Fuels. 2006;**20**:250-256. DOI: 10.1021/ef050163e

[21] Paso K, Kallevik H, Sjoblom J. Measurement of wax appearance temperature using near-infrared (NIR) scattering. Energy & Fuels. 2009;**23**: 4988-4994. DOI: 10.1021/ef900173b

[22] Webber RMJ. Low temperature rheology of lubricating mineral oils: Effects of cooling rate and wax crystallization on flow properties of base oils. Journal of Rheology. 1999;**43**: 911-931. DOI: 10.1122/1.551045

[23] Meighani HM, Ghotbi C, Behbahani TJ, Sharifi K. A new investigation of wax precipitation in Iranian crude oils: Experimental method based on FTIR spectroscopy and theoretical predictions using PC-SAFT model. Journal of Molecular Liquids. 2018;**249**:970-979. DOI: 10.1016/j.molliq.2017.11.110

[24] Rønningsen HP, Bjoerndal B, Hansen AB, Pedersen WB. Wax precipitation from North Sea crude oils. 1. Crystallization and dissolution temperatures, and Newtonian and non-Newtonian flow properties. Energy & Fuels. 1991;**5**:895-908. DOI: 10.1021/ef00030a019

[25] Alcazar-Vara LA, Buenrostro-Gonzalez E. Characterization of the wax precipitation in Mexican crude oils. Fuel Processing Technology. 2011;**92**: 2366-2374. DOI: 10.1016/j.fuproc.2011.08.012

[26] Wessel R, Ball RC. Fractal aggregates and gels in shear flow. Physical Review A: Atomic, Molecular, and Optical Physics. 1992;**46**(6): 3008-3011. DOI: 10.1103/PhysRevA.46.R3008

[27] Soares EJ, Thompson RL, Machado A. Measuring the yielding of waxy crude oils considering its time-dependency and apparent-yield-stress nature. Applied Rheology. 2013;**23**:62798. DOI: 10.3933/ApplRheol-23-62798

[28] Andrade DEV, Da Cruz ACB, Franco AT, Negrão COR. Influence of the initial cooling temperature on the gelation and yield stress of waxy crude oils. Rheologica Acta. 2015;**54**:149-157. DOI: 10.1007/s00397-014-0812-0

[29] Létoffé JM, Claudy P, Kok MV, Garcin M, Volle JL. Crude oils: Characterization of waxes precipitated on cooling by d.s.c. and thermo microscopy. Fuel. 1995;**74**(6):810-817. DOI: 10.1016/0016-2361(94)00006-D

[30] Carlton RA. Polarized light. In: Carlton RA, editor. Pharmaceutical Microscopy. New York: Springer-Verlag New York; 2011. pp. 7-64. DOI: 10.1007/978-1-4419-8831-7

[31] Speight JG. The Chemistry and Technology of Petroleum. 3rd ed. New York: Marcel-Dekker; 1999. 918 p

[32] Pedersen KS, Rønningsen HP. Effect of precipitated wax on viscosity: A model for predicting non-Newtonian viscosity of crude oils. Energy & Fuels. 2000;**14**:43-51. DOI: 10.1021/ef9901185

[33] Li H, Zhang J. A generalized model for predicting non-Newtonian viscosity of waxy crude as a function of temperature and precipitated wax. Fuel. 2003;**82**:1387-1397. DOI: 10.1016/S0016-2361(03)00035-8

[34] Lee HS, Singh P, Thomason WH, Fogler HS. Waxy oil gel breaking mechanisms: Adhesive versus cohesive failure. Energy & Fuels. 2008;**22**(1):480-487. DOI: 10.1021/ef700212v

[35] Chang C, Boger DV, Nguyen QD. Influence of thermal history on the waxy structure of statically cooled waxy crude oil. SPE Journal. 2000;**5**:148-157. DOI: 10.2118/57959-PA

[36] Bai C, Zhang J. Thermal, macroscopic and microscopic characteristics of wax deposits in fields pipelines. Energy & Fuels. 2013;**27**:752-759

[37] Barbato C, Nogueira B, Khalil M, Fonseca R, Gonçalves M, Pinto JC, et al. Contribution to a more reproducible method for measuring yield stress of waxy crude oils emulsions. Energy & Fuels. 2014;**28**(3):1717-1725. DOI: 10.1021/ef401976r

[38] Silva JAL, Coutinho JAP. Dynamic rheological analysis of the gelation behavior of waxy crude oils. Rheologica Acta. 2004;**43**(5):433-441. DOI: 10.1007/s00397-004-0367-6

[39] Oliveira MCK, Texeira A, Vieira LC, Carvalho RM, Carvalho ABM, Couto BC. Flow assurance study for waxy crude oils. Energy & Fuels. 2012;**26**:2688-2695. DOI: 10.1021/ef201407j

[40] Ruwoldt J, Kurniawan M, Oschmann H-J. Non-linear dependency of wax appearance temperature on cooling rate. Journal of Petroleum Science and Engineering. 2018;**165**:114-126. DOI: 10.1016/j.petrol.2018.0 10.1016/j.petrol.2018.02.011 2.011

[41] Kok KM, Létoffé J-M, Claudy P, Martin D, Garcin M, Volle J-L. Comparison of wax appearance temperatures of crude oils by differential scanning calorimetry, thermomicroscopy and viscometry. Fuel. 1996;**75**(7):787-790. DOI: 10.1016/0016-2361(96)00046-4

[42] Srivastava SP, Handoo J, Agrawal KM, Joshi GC. Phase-transition studies in n-alkanes and petroleum-related waxes: A review. Journal of Physics and Chemistry of Solids. 1993;**54**:639-670. DOI: 10.1016/0022-3697(93)90126-C

[43] Guo X, Pethica BA, Huang JS, Prud'homme RK, Adamson DH, Fetters LJ. Crystallization of mixed paraffin from model waxy oils and the influence of micro-crystalline poly(ethylene-butene) random copolymers. Energy & Fuels. 2004;**18**(4):930-937. DOI: 10.1021/ef034098p

[44] Senra M, Panacharoensawad E, Kraiwattanawong K, Singh P, Fogler HS. Role of n-alkane polydispersity on the crystallization of n-alkanes from solution. Energy & Fuels. 2008;**22**:545-555. DOI: 10.1021/ef700490k

[45] Senra M, Scholand T, Maxey C, Fogler HS. Role of polydispersity and co-crystallization on the gelation of long-chained n-alkanes in solution.

Energy & Fuels. 2009;**23**(12):5947-5957. DOI: 10.1021/ef900652e

[46] Dirand M, Bouroukba M, Chevallier V, Petitjean D, Behar E, Ruffier-Meray V. Normal alkanes, multialkane synthetic model mixtures, and real petroleum waxes: Crystallographic structures, thermodynamic properties, and crystallization. Journal of Chemical & Engineering Data. 2002;**47**(2): 115-143. DOI: 10.1021/je0100084

[47] Saxena H, Majhi A, Behera B. Prediction of wax content in crude oil and petroleum fraction by proton NMR. Petroleum Science and Technology. 2018:1-8. DOI: 10.1080/10916466.2018.1536713

[48] Yi S, Zhang J. Relationship between waxy crude oil composition and change in the morphology and structure of wax crystals induced by pour-point-depressant beneficiation. Energy & Fuels. 2011;**25**:1686-1696. DOI: 10.1021/ef200059p

[49] Chen J, Zhang J, Li H. Determining the wax content of crude oils by using differential scanning calorimetry. Thermochimica Acta. 2004;**410**:23-26. DOI: 10.1016/S0040-6031(03)00367-8

[50] Robustillo MD, Coto B, Martos C, Espada JJ. Assessment of different methods to determine the total wax content of crude oils. Energy & Fuels. 2012;**26**:6352-6357. DOI: 10.1021/ef301190s